A RUGGED PRINTED DIPOLE REFERENCE FOR SAR AND FREESPACE MEASUREMENT VERIFICATIONS.

Michael Kanda, Giorgi Bit-Babik, Miguel Richard, and C-K. Chou.
Motorola Corporate EME Research Lab, Fort. Lauderdale, FL, 33322, U.S.A.
Michael.Kanda@motorola.com

INTRODUCTION: The strict regulatory and compliance requirements for SAR and more recently hearing aid compatibility have increased the need for accurate and precise testing methodologies. This is also required for conforming to quality management accreditation guidelines such as ISO/IEC 17025. Though rigorous steps are taken to assure that every instrument in the testing process is within strict specifications, system verification is the fundamental way to assure that the total system is operating within specification. System verification promotes accurate and precise measurements by verifying the measurement repeatability of a reference source on a daily basis. A conventional tuned half wave dipole is recommended in the standards [1 – 3]. A much more cost effective and robust printed dipole as an alternative reference for daily system verification was proposed in [4]. Calibrated commercial dipoles can cost as much as $2,500. The printed dipole costs a small fraction of the amount. The ruggedness of the printed dipole allows for use in factory and product development environments.

OBJECTIVE: This study expands the original report [4,5] by providing design guidelines and reference SAR and freespace values for the printed dipole. Freespace evaluation is important for freespace measurement standards like hearing aid compliance [3]. Validation of parameters such as surface detection accuracy and probe retraction errors are difficult in the SAM phantom due to the complex contours of the surface. Complex contours can be integrated into the printed dipole for fast and repeatable positioning on complex surfaces, like the SAM head phantom.

DESIGN GUIDELINES: The dipole is constructed by etching the balun on a substrate with copper on both sides. A Hitachi material was selected for the dipoles. The material is similar to FR-4 but with lower loss ($\varepsilon_r = 4.3$, $\tan\delta = 0.008$). The dipole arms are etched on opposite sides of the substrate as shown in Figure 1.

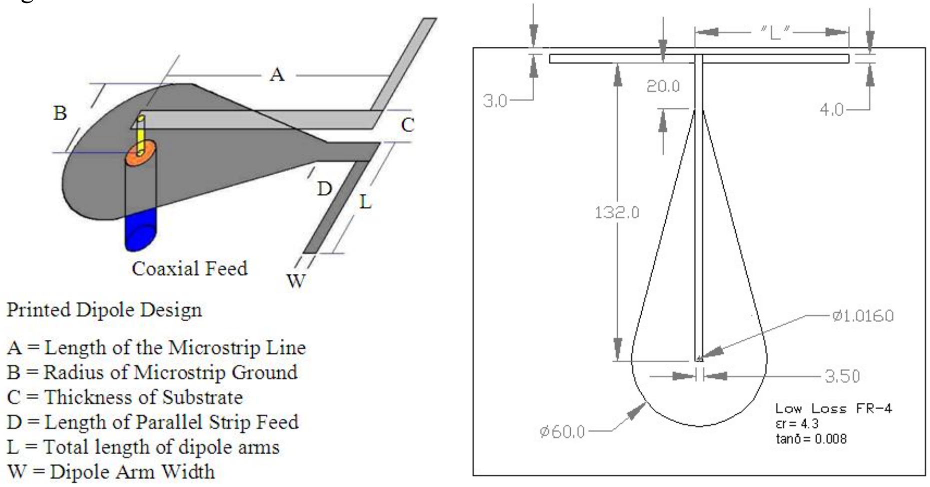

Figure 1 – Printed dipole configuration.

The broadband balun was selected so tuning is achieved by adjusting the length of the dipole arms (L) while the dimensions of the balun remain unchanged. The length "L" is defined as the distance from the tip of the arm to the opposite side of the parallel feed line. The dipole behaves like a thick wire dipole with resonant length is significantly less than λ/2. Simple relations to determine the appropriate dipole arm length for a given resonant frequency are shown in Fig 2. The SAR dipole lengths approach the freespace dipoles as the electrical length between the dipole and the liquid increases.

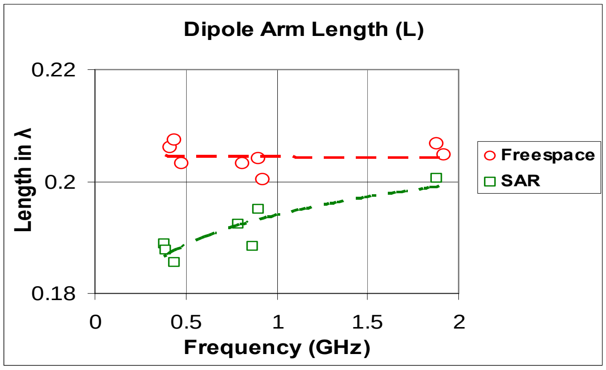

$$L_{free} = 0.204\lambda_0$$

$$L_{SAR} = 0.194 f^{0.05} \lambda_0$$

$$f = frequency(GHz)$$

Figure 2 – Dipole arm length (L) for various frequencies.

RESULTS: The antennas exhibit roughly a 10% bandwidth similar to a conventional dipole with return loss generally better than -15 dB. Good freespace balance was observed around 900 MHz but degradation was seen in E-field balance at 1880 as shown in Figure 3. The unbalance was confirmed numerically using CST Microwave Studios, shown in Figure 4. The unbalance is undesirable but is suspected to be good enough to allow use of this balun for reference measurements at these frequencies. Similar results were seen with SAR dipoles.

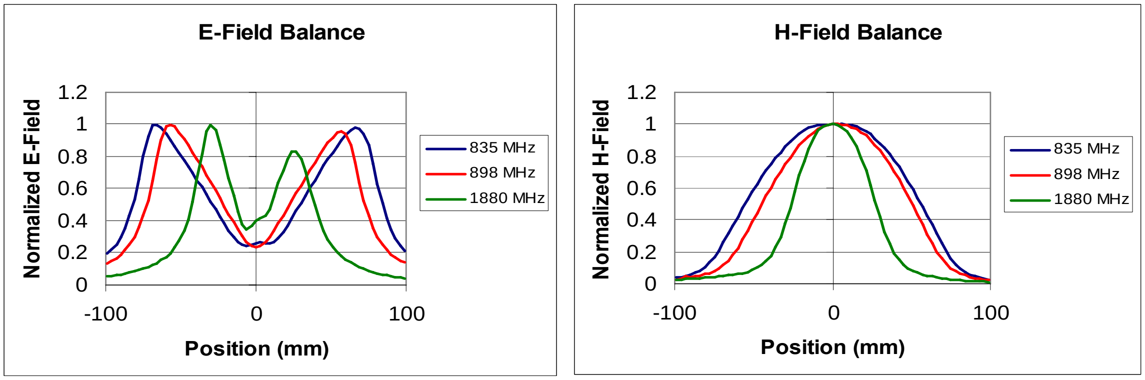

Figure 3 – Normalized freespace E and H-field balance

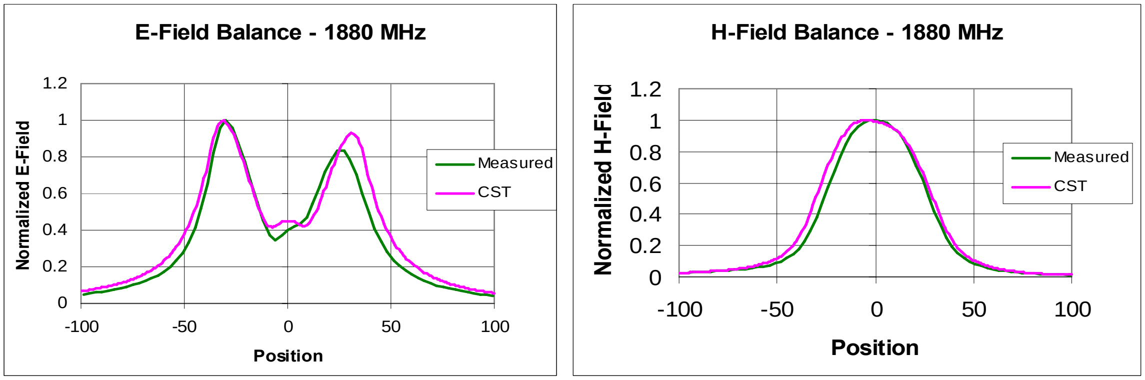

Figure 4 – Numerical and measured balance at 1880 MHz

REFERENCE VALUES – The dipole was modeled in XFDTD and CST to determine SAR and freespace reference values, (XFDTD example shown in Figure 5). When compared to measurement, good consistency was seen across the frequencies of interest. Following the respective standards, reference values were determined for a 10mm distance for freespace and 15 mm distance for 800/900 MHz SAR and 10mm distance for 1880 MHz SAR.

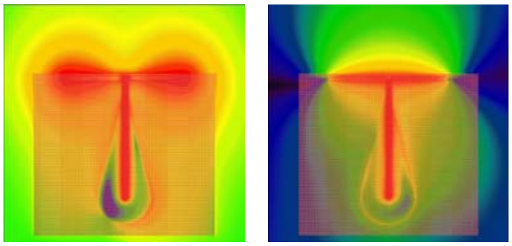

Figure 5 – Freespace E and H-field measurements of the 898 MHz dipole

Good correlation was seen between the results of the measurements and numerical modeling (XFDTD and CST) of the freespace dipoles, shown in Tables 1 and 2.

Table 1 - Freespace results for 100 mW input RMS, (for measurements, N=8, 9)

Freq	XFDTD E	Meas E	% Diff	XFDTD H	Meas H	% Diff	% Stdev E	% Stdev H
813	224.8	206.6	-8.1%	513.9	497.3	-3.2%	6.3%	6.8%
835	214.9	198.8	-7.5%	495.4	477.3	-3.7%	6.0%	3.3%
898	213.2	200.0	-6.2%	503.2	498.9	-0.8%	5.9%	4.4%
1880	153.6	144.5	-5.9%	447.8	447.4	-0.1%	5.5%	4.0%

Table 2 - XFDTD Comparison with CST

Freq	XFDTD E	CST E	% Diff	XFDTD H	CST H	% Diff
813	224.8	236.4	-5.1%	513.9	522.6	-1.7%
835	214.9	232.2	-8.0%	495.4	516.4	-4.2%
898	213.2	220.9	-3.6%	503.2	500.5	0.5%
1880	153.6	149.3	2.8%	447.8	403.5	9.9%

Good correlation was also seen for both 1 and 10 g SAR measurements, as shown in Table 3.

Table 3 - SAR Results, 1W normalized SAR values

Frequency	1g XFDTD	10g XFDTD	1g Meas	10g Meas	1g % Diff	10g % Diff
813	9.08	5.90	N/A	N/A	N/A	N/A
835	9.20	5.97	8.95	5.85	2.7%	2.0%
898	10.08	6.50	9.75	6.35	3.3%	2.4%
1880	31.11	16.03	32.6	17.1	-4.8%	-6.7%

REPEATABILITY IN SAM – Incorporation of the contour allows for easy conformal positioning of the dipole to the SAM phantom. Four different dipoles were generated to test different locations in the phantom.

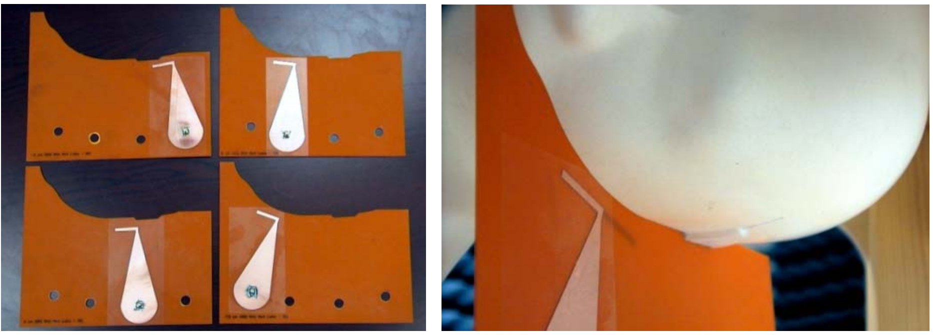

Figure 6 – Set of conformal dipoles at varying distances from the ear reference point.

Currently only flat phantom validations are possible. These dipoles allow for system verification in the SAM phantom which allows for verification of the surface detection mechanism. The positioning repeatability was determined by taking a series of measurements with repositioning (denoted as "Positioning" in the table) the dipole between each run. The histogram of the results is shown in Fig.6. The measurement repeatability ("Measurement") was determined by taking a series of measurements without repositioning the dipole. The overall positioning repeatability ("Adj Positioning") was determined by isolating the positioning repeatability from the measurement repeatability (both were considered independent): $Adj\ Positioning = \sqrt{Positioning^2 - Measurement^2}$

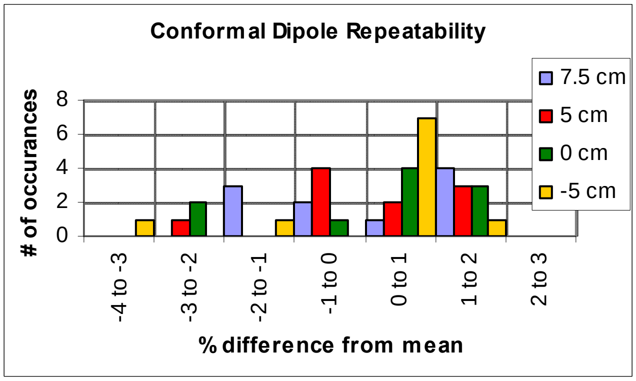

Figure 6 – Positioning repeatability of the conformal dipoles.

When compensated for the measurement repeatability, the overall positioning repeatability ("Adj. Positioning") was found to be within a standard deviation of less than +/- 2% was observed for 4 locations in the SAM phantom as shown in Table 4.

Table 4 - Positioning Repeatability (% Stdev)

	7.5 cm	5 cm	0 cm	-5 cm
Positioning	1.1%	1.2%	1.5%	1.6%
Measurement	0.7%	1.0%	0.4%	0.3%
Adj. Positioning	0.9%	0.6%	1.4%	1.6%

CONCLUSION: This study showed that a printed dipole can be designed to have performance characteristics comparable to typical system verification dipoles meeting the requirements of the standards. The printed dipoles have added advantages of being low cost, robust, and easily tunable for use with other frequencies or tissue simulating tissue liquids. The printed dipole can also incorporate spacers that allow for accurate and precise positioning in flat and the complex SAM phantom.

REFERENCES

[1] IEEE, "IEEE Recommended Practice for Determining the Peak Spatial-Average Specific Absorption Rate (SAR) in the Human Head from Wireless Communications Devices: Measurement Techniques," IEEE Standard 1528, 2003.

[2] European Committee for Electrotechnical Standardization (CENELEC), "Basic standard for the measurement of Specific Absorption Rate related to human exposure to electromagnetic fields from mobile phones (300 MHz -3 GHz)," CENELEC EN 50361, 2001.

[3] ANSI, "ANSI National Standard for Methods of Measurement of Compatibility between Wireless Communications Devices and Hearing Aids," ANSI-PC63.19-2001, Revision 3.1. DRAFT.

[4] M. Richard, M. Kanda, G. Bit-Babik, C. DiNallo, CK Chou. A Rugged Microstrip Printed Dipole Reference for SAR System Verification. IEEE MTT-S International Microwave Symposium, Seattle, WA. June 2-7, 2002.

[5] M. Gans, et al., "Frequency Independent Balun," IEEE Proc., vol.53, June 1965, pp. 647 – 648.